

International Journal of Modern Physics D
 © World Scientific Publishing Company

THE POLARIMETRIC MULTI-FREQUENCY RADIO SOURCES PROPERTIES

VINCENZO GALLUZZI

*INAF, Osservatorio di Radioastronomia, Via Gobetti 101
 Bologna, 40129, Italy
 vgalluzzi@ira.inaf.it*

*Dipartimento di Fisica e Astronomia, Università di Bologna, via Ranzani 1
 Bologna, 40126, Italy
 vincenzo.galluzzi@unibo.it*

MARCELLA MASSARDI

*INAF, Osservatorio di Radioastronomia, Via Gobetti 101
 Bologna, 40129, Italy
 massardi@ira.inaf.it*

Received Day Month Year
 Revised Day Month Year

The polarization properties of extragalactic radio sources at frequencies higher than 20 GHz are still poorly constrained. However, their characterization would provide invaluable information about the physics of the emission processes and is crucial to estimate their contamination as foregrounds of the polarized cosmic microwave background (CMB) angular power spectrum on scales $\lesssim 30$ arcmin. In this contribution, after summarizing the state-of-the-art of polarimetric observations in the millimetric wavelength bands, we present our observations of a complete sample of 53 sources with $S_{20\text{ GHz}} > 200$ mJy carried out with the Australia Telescope Compact Array between 5.5 and 38 GHz. The analysis clearly shows that polarization properties cannot be simply inferred from total intensity ones, as the spectral behaviors of the two signals are typically different.

Keywords: radio galaxies; polarization; cosmic microwave background.

PACS numbers:

1. The state-of-the-art in polarimetric observations

Bright extragalactic radio source samples are mostly associated to the nuclei of active galaxies. A widely held view is that their spectra result from a superposition of a number of compact regions of different sizes, self-absorbed at different frequencies (e.g. see Ref. 1 and Ref. 2 for a review), associated to knot-like Doppler-boosted structures along a relativistic jet, powered by the central nuclear activity.³

The characterization of the total intensity emission for large samples of radio

source population is only a recent achievement, and still open to discussion. Wide-area surveys are necessary to achieve statistics on the bright less numerous samples, while high sensitivity is needed to explore the faintest samples. Only the former were available in the catalogs extracted from full-sky maps from satellite missions like WMAP (with a completeness limit of $\simeq 1$ Jy at 23 GHz⁴⁻⁷) and Planck (with a completeness limit of $\simeq 500$ mJy at 30 GHz⁸). New broad-band correlators made high sensitivity available for interferometric observations up to the mm and sub-mm regimes, allowing wide-area deep surveys to be carried out also from the ground at frequencies above ~ 10 GHz. Thus, the Australia Telescope 20 GHz (AT20G) Survey^{9,10} covered the full Southern sky with 91% completeness above 100 mJy and 79% completeness above 50 mJy in regions south of declination -15° .

By combining the ground- and satellite-based instrumental capabilities, several authors¹¹⁻¹⁴ recently provided a broad-band view of the total intensity emission of the bright radio source population: it seems to be dominated by relatively young compact objects. A double power-law model is adequate to describe spectral behaviors for more than 2 decades in frequency: this indicates that a single dominant component is responsible for the (typically optically thin) emission above ~ 30 GHz. Emission is typically variable: objects brighter than 500 mJy (at 20 GHz) on average vary their flux density (at 20 GHz) more than 6% over a 6 months lag, and the rate grows with frequency.

The study of the polarized emission both in frequency and space would help describing the dynamics of the jets. Synchrotron emission of each component is intrinsically highly linearly polarized¹⁵ (up to 70 – 80%) but typically observed integrated polarized fractions for compact extragalactic radio sources are rarely as high as $\sim 10\%$. They are, in fact, the result of vector averaging along the line of sight (depolarization is mostly induced by differential Faraday rotation),¹⁶ within the observing resolution element (in this case unresolved magnetic sub-structures cause depolarization), and within the band of the polarized components emission. Hence, polarimetric observations typically still constitute an observational challenge because of the requested high sensitivity, calibration accuracy, and the detailed knowledge of instrumental properties and systematics (see Massardi *et al.* in this volume). Table 1 lists some of the available multi-frequency compilations, surveys and complete samples follow-up that include polarimetric information: it does not claim to be an exhaustive picture and aims to trace the basic references in the following discussion.

For the above mentioned reasons, our current knowledge of polarimetric properties of radio sources mostly rely on < 10 GHz selected samples including the NVSS survey²⁶ that covered the full sky above -45° , remaining complete down to 2.5 mJy in total intensity and with $\sigma_P \sim 0.2$ mJy in polarized emission.

Table 1. Summary of some of the surveys in polarization available at radio frequencies (update to Table 3 in Tucci *et al.*,⁴¹ 2004).

References	Frequency (GHz)	# sources	Notes
Eichendorf & Reinhardt (1979) ¹⁷	[0.4, 15]	510	compilation of multi-frequency data
Tabara & Inoue (1980) ¹⁸	[0.4, 10.7]	1510	compilation of multi-frequency data
Simard-Normandin <i>et al.</i> (1981) ^{19, 20}	[1.6, 10.5]	555	compilation of multi-frequency data
Perley (1982) ²¹	1.5, 4.9	404	compilation of multi-frequency data
Rudnick <i>et al.</i> (1985) ²²	[1.4, 90]	20	compilation of multi-frequency data
Aller <i>et al.</i> (1992) ²³	4.8, 8.0, 14.5	62	90% complete sample with $S_{5\text{ GHz}} > 1.3\text{ Jy}$
Okudaira <i>et al.</i> (1993) ²⁴	10	99	flat-spectrum sources with $S_{5\text{ GHz}} > 0.8\text{ Jy}$
Nartallo <i>et al.</i> (1998) ²⁵	273	26	compilation of flat-spectrum radio sources
Condon <i>et al.</i> (1998) - NVSS ²⁶	1.4	$\sim 2 \times 10^6$	100% complete survey down to $S_{1.4\text{ GHz}} > 2.5\text{ mJy}$
Aller <i>et al.</i> (1999) ²⁷	4.8, 8.0, 14.5	41	BLLac sources
Fanti <i>et al.</i> (2001) ²⁸	4.9, 8.5	87	CSS sample with $S_{0.4\text{ GHz}} > 0.8\text{ Jy}$
Lister (2001) ²⁹	43	32	90% complete sample with $S_{5\text{ GHz}} > 1.3\text{ Jy}$
Klein <i>et al.</i> (2003) ³⁰	1.4, 2.7, 4.8, 10.5	192	compilation of detections of the B3-VLA survey
Ricci <i>et al.</i> (2004) ³¹	18.5	250	complete sample with $S_{5\text{ GHz}} > 1\text{ Jy}$
Jackson <i>et al.</i> (2007) ³²	8.4	~ 16000	JVAS-CLASS surveys
Massardi <i>et al.</i> (2008) AT20G-BSS ¹¹	4.8, 8.6, 20	320	AT20G bright sample
Lopez-Caniego <i>et al.</i> (2009) ³³	23, 33, 41	22	polarization detections in WMAP maps
Jackson <i>et al.</i> (2010) ³⁴	8.4, 22, 43	230	WMAP sources follow-up
Murphy <i>et al.</i> (2010) AT20G ⁹	4.8, 8.6, 20	5890	93% complete survey with $S_{20\text{ GHz}} > 40\text{ mJy}$
Trippe <i>et al.</i> (2010) ³⁵	[80, 267]	86	complete sample with $S_{90\text{ GHz}} > 0.2\text{ Jy}$
Battye <i>et al.</i> (2011) ³⁶	8.4, 22, 43	230	WMAP sources follow-up
Sajina <i>et al.</i> (2011) ¹²	4.8, 8.4, 22, 43	159	AT20G sources follow-up
Massardi <i>et al.</i> (2013) ³⁷	4.8, 8.6, 18	193	complete sample with $S_{20\text{ GHz}} > 500\text{ mJy}$
Agudo <i>et al.</i> (2014) ³⁸	86, 229	211	complete sample of flat-spectrum sources with $S_{86\text{ GHz}} > 1\text{ Jy}$
Planck Collaboration (2015) ⁸	30, 44, 70	122, 30, 34	polarization detections in Planck LFI maps (PCCS2)
	100, 143, 217, 353	20, 25, 11, 1	polarization detections in Planck HFI maps (PCCS2)

Noticeable exceptions are few high frequency-selected samples that are typically limited to flat-spectrum or bright objects.

The polarization of WMAP sources has been investigated by López-Caniego *et al.* (2009, Ref. 33) by using WMAP data: 14 extragalactic objects were significantly detected in polarization. Slightly larger samples were detected in the Planck maps and recorded in the “Planck Catalogue of Compact Sources”⁸ (PCCS, 2nd version), listing 122 detections down to a minimum polarized flux density of 117 mJy at 30 GHz but complete only to 0.6 Jy. Ground-based follow-up observations of a complete sample of 203 WMAP sources were carried out with the VLA by Jackson *et al.* (2010, Ref. 34) and Battye *et al.* (2011, Ref. 36): polarized emission was detected for 123, 169 and 167 objects at 8.4, 22 and 43 GHz, respectively.

The Plateau de Bure Interferometer (PdBI) observations of Trippe *et al.* (2010, Ref. 35) of a $S_{90\text{ GHz}} > 200\text{ mJy}$ complete sample of 86 sources found an average fractional polarization level of $\simeq 2 - 7\%$, higher for BLLac ($\simeq 7\%$) than for QSO ($\simeq 5\%$) or Seyfert galaxies ($\simeq 3\%$). The size scales relevant for the polarization emission measurements are found to be comparable to those of interest for total intensity flux density measurements.

The full AT20G catalog^{9,10} includes the 20 GHz polarized intensity for 768 sources, 467 of which also have simultaneous polarization detections at 5 and/or 8 GHz, out of a total of 5890 sources. The detection limit is defined as $\max(3\sigma, 0.01S_{20\text{ GHz}}, 6\text{ mJy})$. Sadler *et al.* (2006, Ref. 39) presented polarization measurements for a sample of 173 AT20G sources brighter than $S_{20\text{ GHz}} = 100\text{ mJy}$: 129 ($\simeq 75\%$) were detected at 20 GHz, with a median fractional polarization of 2.3%. Massardi *et al.* (2008, Ref. 11) discussed the polarization properties of the AT20G bright sample ($S_{20\text{ GHz}} \geq 500\text{ mJy}$), finding 213 polarization detections ($\geq 3\sigma$) at 20 GHz out of a total of 320 sources ($\simeq 67\%$), with a median fractional polarization of 2.5% at 20 GHz (confirmed also by Refs. 34, 36). The spectral indices in total intensity and in polarization were found to be similar on average, but there were several objects for which the spectral shape of the polarized emission is substantially different from the spectral shape in total intensity. Several studies of radio source polarization, mostly for samples selected at 1.4 GHz and dominated by steep-spectrum objects, have reported indications that the polarization degree increases with decreasing flux density.⁴⁰⁻⁴⁴ Massardi *et al.* (2013, Ref. 37) analyzed high-sensitivity polarization observations (in the 4.8 – 20 GHz frequency range) of a complete AT20G bright ($S_{20\text{ GHz}} > 500\text{ mJy}$) source sub-sample and found no statistically significant relationship between the polarization fraction and the total intensity flux density, and no clear indication of trends of fractional polarization with frequency, up to 20 GHz.

Sajina *et al.* (2011, Ref. 12) obtained polarization measurements with the VLA at 4.86, 8.46, 22.46, and 43.34 GHz of 159 out of the ~ 200 AT20G radio galaxies with $S_{20\text{ GHz}} \geq 40\text{ mJy}$ in an equatorial field of the Atacama Cosmology Telescope survey: polarized flux was detected at $> 95\%$ confidence level for 141, 146, 89, and 59 sources, from low to high frequencies. The measured polarization fractions are

typically $< 5\%$, although in some cases they are measured to be up to $\simeq 20\%$. They find indications of increasing polarization fraction with frequency (confirmed also by Ref. 45 in the 15 – 90 GHz range and by Ref. 38 in the 86 – 229 GHz range). This trend is stronger for steeper spectrum sources as well as for the lower flux density sources.

Finally, it has been argued that the ordering of magnetic fields should increase in the inner regions, giving a higher polarization degree at higher frequency,⁴¹ while Faraday depolarization should affect more the lower frequency observations.

However, it seems clear that extrapolations from low frequencies (< 20 GHz) or from total intensity emission are inadequate to model the radio source contribution in CMB polarization maps (see Ref. 46) and that future surveys will benefit CMB polarization experiments by statistically characterizing radio source populations down to lower flux density limits. On the one hand, in fact, foreground sources are expected to be the most relevant contaminant of the CMB angular power spectrum for angular scales up to ~ 30 arcmin in the 70 – 100 GHz frequency range, where Galactic foregrounds (Galactic synchrotron and thermal dust emissions) are, instead, at a minimum. On the other hand, radio mm-band facilities have reached so far sensitivities that, in principle, are useful to constraining models that predict cosmic polarization rotation (CPR), as a result of violations of fundamental principles (such as the Einstein Equivalence Principle, the Lorentz Invariance or the CPT symmetry),^{47–49} at the same level or even better than constraints coming from CMB observations.⁵⁰ Furthermore, multi-steradian samples of high frequency-selected polarized sources are also important for identifying suitable calibrators for CMB polarimetric experiments and upcoming millimeter-wave telescopes. See Mascardi *et al.* in this volume for a short review about the role of radio sources in polarimetric cosmological investigations.

Broad frequency range and multi-epoch observations of low flux density-limited samples are now needed to complement the view of radio source population properties in polarization and provide samples useful for cosmological studies, like those that are being carried out in the framework of the Planck-ATCA Co-eval Observations project¹⁴ for a $S_{20\text{GHz}} > 200$ mJy sample selected in the AT20G catalog. The project is briefly summarized in the following section.

2. The Planck-ATCA Co-eval Observations project

The Planck-ATCA Co-eval Observations (PACO, Refs. in 51, 52, 53, 14) project, carried out with the Australia Telescope Compact Array (ATCA), observed 464 objects drawn from the Australia Telescope survey at 20 GHz (AT20G, Refs. in 9, 10) between 4.5 and 40 GHz (below and overlapping with the two lower *Planck* frequency bands) in 65 epochs during the period July 2009–August 2010, corresponding to the first two sky surveys of the satellite nominal mission. Source were scheduled for ATCA and Planck observations to occur within 10 days of each other in order to minimize source variability effects. The sample is made of 3 partially

overlapping sub-samples, namely the *bright sample* ($S_{20\text{ GHz}} > 500\text{ mJy}$), the *faint sample* ($S_{20\text{ GHz}} > 200\text{ mJy}$) and the *spectrally-selected sample*, plus one of potentially strongly variable objects identified among the ATCA calibrators database.

The main goal of the project was to characterize the radio source population observed by the Planck satellite down to well below its detection limits (down to a factor of 5) in a broad frequency range and on different epochs. Thanks to the combination of ATCA and Planck detected flux densities, we reconstructed the spectral properties of the sources in the 5 – 217 GHz frequency range. The vast majority ($\simeq 91\%$) of the sources show a remarkably smooth spectrum, well described by a double power law over the whole range. This translates in several compact objects showing a peaked spectrum with an optically thin steep behavior for frequencies $\gtrsim 30\text{ GHz}$, probably associated to recently emitted components. This turns at odds with the criterion, well established at cm-wavelengths, according to which flat spectra are usually associated to compact sources while steep emitted synchrotron is indicative of extended sources. No further synchrotron break is observed at high frequencies. Assuming a continuous injection model,^{54,55} our finding can be considered an indication that the sources are young, i.e. τ_{syn} no more than 10^{3-4} yr .¹⁴

2.1. Polarimetric follow-up

In September 2014 a high sensitivity ($\sigma_P \simeq 0.2\text{ mJy}$) polarimetric observation in 3 correlator spectral setups (that allow $2 \times 2\text{ GHz}$ simultaneous bands centered at 5.5 – 9, 18 – 24 and 33 – 38 GHz) was performed with ATCA (Massardi, project C2922) for a complete sub-sample of 53 extragalactic compact radio sources of the faint ($S_{20\text{ GHz}} > 200\text{ mJy}$) PACO sample,⁵² covering the Southern Ecliptic Pole region (ecliptic latitude $< -75^\circ$).

The choice of the region of the sky was motivated in PACO project by the Planck scanning strategy, which gives maximum sensitivity near the ecliptic poles.

The array configuration was the H214, an hybrid with a nominal spatial resolution ($\simeq \lambda/b_{\text{max}}$) that spans from 8 to 55 arcsec for the observed frequencies.^a All the objects in the sample are point-like.

The project was allocated in 12 h (*i.e.* $\simeq 4\text{ h}$ per band, including overheads and calibration), during which weather conditions were very good. Every object has been observed for each spectral setup at least for $2 \times 1.5\text{ min}$ cuts, that is estimated to be enough to reach the theoretical noise level of 0.2 mJy in polarized emission.

Data reduction was performed with MIRIAD software following standard polarimetric calibration procedures.^b The outcome are high sensitivity spectral profiles in total intensity and polarization (some of them are reported in Fig. 1, together with past PACO and AT20G observations available). The detection rate in polarization is about 90% at 5σ .

^aIndeed, taking into account the longest baseline with the sixth antenna ($\simeq 4.5\text{ Km}$) the spatial resolution spans from 0.4 to 2.5 arcsec but in this case the achievable sensitivity is reduced.

^bAccording to ATCA Users' Guide: www.narrabri.atnf.csiro.au/observing/users_guide.

Similar to what was found in past analysis, about 96% of the objects total intensity behavior can be fitted with a double power law. Polarimetric spectra, instead, typically show a different and sometimes more complex behavior with respect to total intensity (see Fig. 1), in agreement with Massardi *et al.* findings (2013, Ref. 37). As found in total intensity, a steepening of spectra is observed at higher frequencies both in total intensity and in polarization. The median fractional polarization is $\simeq 2.1\%$ at 18 GHz (in agreement with Refs. 39, 11, 36). A tiny trend with frequency is observed for the whole sample (see Fig. 2). A comprehensive analysis of the data, including spectral classifications and source counts in polarization will be presented in a future paper (Galluzzi *et al.*, in preparation).

The project will be complemented by a second observational session scheduled with ATCA in March 2016 to observe 106 sources in the faint PACO sample with ecliptic latitude $< -65^\circ$ (i.e. including the 53 already observed in the previous epoch) at all the already observed frequencies and to extend down to $\simeq 2$ GHz, and by an ALMA Cycle-3 project, accepted with high-ranking, to re-observe a complete sub-sample of 31 objects at $\simeq 100$ GHz, that will provide interesting hints for cosmological applications, as described in Massardi *et al.* (this volume).

3. Cosmological outreach

As already stressed in the first section, extrapolations from low frequencies (< 20 GHz) are inadequate to model the radio source contribution in CMB polarization maps⁴⁶ and future surveys will benefit CMB polarization experiments by statistically characterizing radio source populations, as those proposed in our ALMA-Cycle 3 proposal. Moreover those stable, brighter and highly polarized sources of our sample are potentially of interest as calibrators for many ground-based facilities looking for primordial B-modes in the CMB angular power spectrum or cosmic polarization rotation, for which a clear detection has not been claimed so far and available upper limits are about 1° .⁴⁹ Indeed, recently the POLARBEAR Collaboration reports for the first time a sub-degree upper limit (see Ref. 50). From our data we can assess a total error on polarization angle of $\simeq 3^\circ$, by assuming that the calibration error for polarized fluxes (estimated $\simeq 10\%$) is equally distributed among Stokes parameter Q and U . However, recent measurements of polarization angles performed with VLA and ATCA are found to be in agreement within $\pm 2^\circ$,⁵⁹ which is a current conservative estimate of the absolute calibration error on this quantity.

4. Acknowledgments

We acknowledge financial support by the Italian *Ministero dell'Istruzione, Università e Ricerca* through the grant *Progetti Premiali 2012-iALMA* (CUP C52I13000140001). We thank the anonymous referee for the useful comments. We thank the staff at the Australia Telescope Compact Array site, Narrabri (NSW), for the valuable support they provide in running the telescope and in data reduction. The Australia Telescope Compact Array is part of the Australia Telescope which is

8 VINCENZO GALLUZZI, MARCELLA MASSARDI

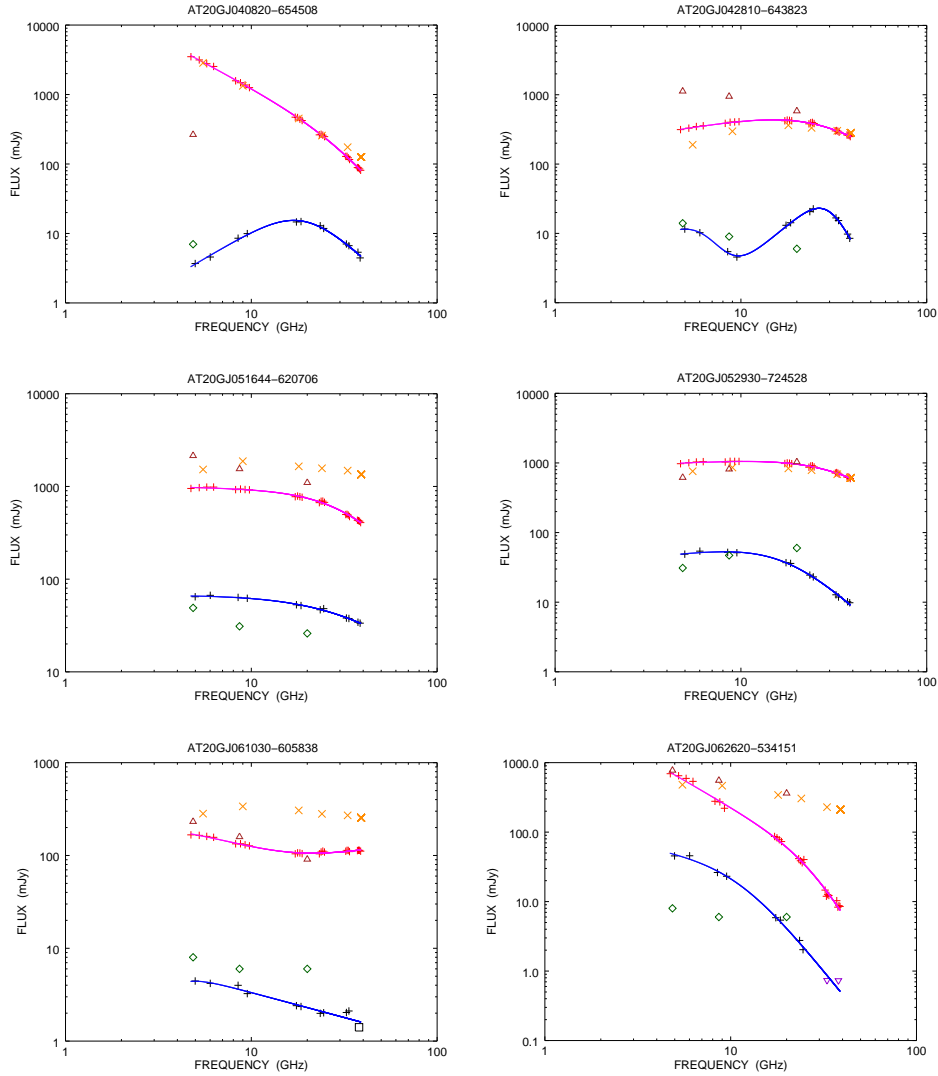


Fig. 1. Spectra in total intensity and polarization (error bars are not displayed since they are smaller than plotting symbols) for some sources drawn from the 53 of the faint PACO sample, observed in September 2014. **Total intensity:** red crosses indicate total intensity ATCA September 2014 observations (each point represents a 512 MHz-bin) and magenta solid lines indicate fitting curves. Median PACO flux densities (July 2009–August 2010) are indicated with orange “x”. AT20G observations (best epoch in 2004–2008) are reported with brown triangles. **Polarization:** black crosses and black squares indicate September 2014 observations (each point represents a 1 GHz-bin and the 2 GHz-full bandwidth, respectively) and blue solid lines indicate fitting curves. AT20G observations (best epoch in 2004–2008) are reported with green diamonds. Upper limits are shown as violet downwards triangles.

funded by Commonwealth of Australia for operation as a National Facility managed by CSIRO.

References

1. A. P. Marscher, *Nature* **288** (1980) 12
2. G. De Zotti, M. Massardi, M. Negrello and J. Wall, *A&A Rev.* **18** (2010) 1
3. R. D. Blandford and A. Königl, *ApJ* **232** (1979) 34
4. F. Argüeso, J. González-Nuevo and L. Toffolatti, *ApJ* **598** (2003) 86
5. G. De Zotti, R. Ricci, D. Mesa *et al.*, *A&A* **431** (2005) 893
6. E. L. Wright, X. Chen, N. Odegard *et al.*, *ApJS* **180** (2009) 283
7. B. Gold *et al.*, *ApJS* **192** (2011) 15
8. Planck Collaboration, arXiv:1507.02058 (2015)
9. T. Murphy *et al.*, *MNRAS* **402** (2010) 2403
10. M. Massardi, R. D. Ekers, T. Murphy *et al.*, *MNRAS* **412** (2011) 318
11. M. Massardi, R. D. Ekers, T. Murphy *et al.*, *MNRAS* **384** (2008) 775
12. A. Sajina *et al.*, *ApJ* **732** (2011) 45
13. X. Chen, J. P. Rachen, M. López-Caniego *et al.*, *A&A* **553** (2013) A107

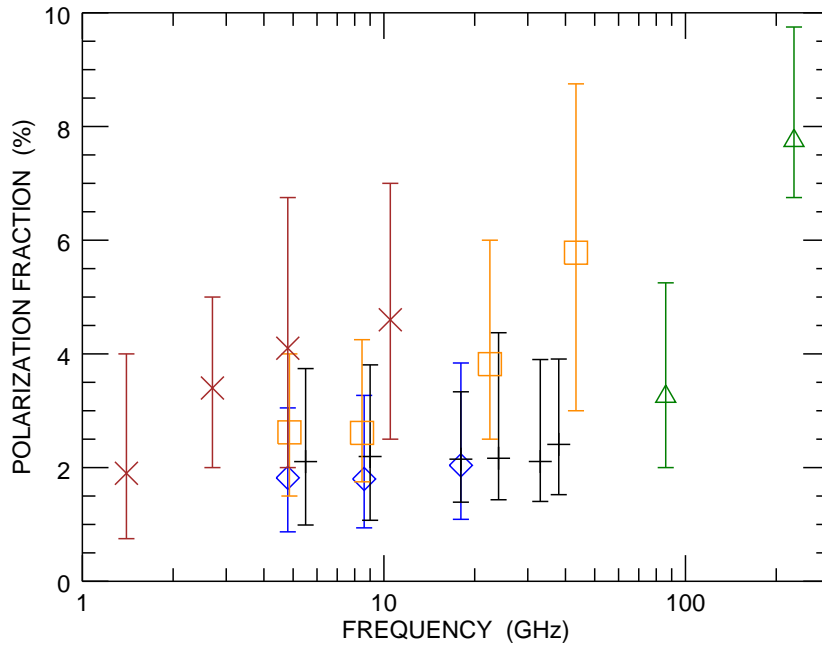


Fig. 2. Median fractional polarizations (error bars report inter-quartile distances) at different frequencies for our observations (black crosses) and some other samples (reported also in the table 1): the AT20G survey⁹ (blue diamonds), Klein *et al.*³⁰ (red “x”), Agudo *et al.*³⁸ (green triangles), and Sajina *et al.*¹² (orange squares).

10 VINCENZO GALLUZZI, MARCELLA MASSARDI

14. M. Massardi *et al.*, *MNRAS* **455**(3) (2015) 3249
15. V. L. Ginzburg and S. I. Syrovatskii, *ARA&A* **7** (1969) 375
16. B. J. Burn, *MNRAS* **133** (1966) 67
17. W. Eichendorf and M. Reinhardt, *Ap&SS* **61** (1979) 153
18. H. Tabara and M. Inoue, *A&AS* **39** (1980) 379
19. M. Simard-Normandin, P. P. Kronberg and J. Neidhoefer, *A&AS* **43** (1981) 19
20. M. Simard-Normandin, P. P. Kronberg and S. Button, *ApJS* **46** (1981) 239
21. R. A. Perley, *AJ* **87** (1982) 859
22. L. Rudnick, T. W. Jones, H. D. Aller *et al.*, *ApJS* **57** (1985) 693
23. M. F. Aller, H. D. Aller and P. A. Hughes, *ApJ* **399** (1992) 16
24. A. Okudaira, H. Tabara, T. Kato and M. Inoue, *PASJ* **45** (1993) 153
25. R. Nartallo *et al.*, *MNRAS* **297** (1998) 667
26. J. J. Condon, W. D. Cotton, E. W. Greisen *et al.*, *AJ* **115** (1998) 1693
27. M. F. Aller, H. D. Aller and P. A. Hughes, *BAAS* **31** (1999) 1397
28. C. Fanti, F. Pozzi, D. Dallacasa *et al.*, *A&A* **369** (2001) 380
29. M. L. Lister, S. J. Tingay and R. A. Preston, *ApJ* **554** (2001) 964
30. U. Klein, K.-H. Mack, L. Gregorini and M. Vigotti, *A&A* **406** (2003) 579
31. R. Ricci, I. Prandoni, C. Gruppioni *et al.*, *A&A* **415** (2004) 549
32. N. Jackson, R. A. Battye, I. W. A. Browne *et al.*, *MNRAS* **376** (2007) 371
33. M. López-Caniego, M. Massardi, J. González-Nuevo *et al.*, *ApJ* **705** (2009) 868
34. N. Jackson *et al.*, *MNRAS* **401** (2010) 1388
35. S. Trippe, R. Neri, M. Krips *et al.* *A&A* **515** (2010) A40
36. R. A. Battye *et al.*, *MNRAS* **413** (2011) 132
37. M. Massardi, S. G. Burke-Spolaor, T. Murphy *et al.*, *MNRAS* **436** (2013) 2915
38. I. Agudo, C. Thum, J. L. Gómez and H. Wiesemeyer, *A&A* **566** (2014) A59
39. E. M. Sadler *et al.*, *MNRAS* **371** (2006) 898
40. D. Mesa, C. Baccigalupi, G. De Zotti *et al.*, *A&A* **396** (2002) 463
41. M. Tucci *et al.*, *MNRAS* **349** (2004) 1267
42. A. R. Taylor, J. M. Stil, J. K. Grant *et al.*, *ApJ* **666** (2007) 201
43. J. K. Grant, A. R. Taylor, J. M. Stil *et al.* *ApJ* **714** (2010) 1689
44. R. Subrahmanyan *et al.*, *MNRAS* **402** (2010) 2792
45. I. Agudo, C. Thum, H. Wiesemeyer and T. P. Krichbaum, *ApJS* **189** (2010) 1
46. QUIET Collaboration, arXiv:1412.1111 (2014)
47. W-T Ni, *Prog. Theor. Phys. Suppl.* **172** (2008) 49
48. V. A. Kostelecký and M. Mewes, *Phys. Rev. D* **80** (2009) 015020
49. S. di Serego Alighieri, *Int. J. Mod. Phys. D* **24** (2015) 1530016
50. POLARBEAR Collaboration, arXiv:1509.02461 (2015)
51. M. Massardi *et al.*, *MNRAS* **415** (2011) 1597
52. L. Bonavera *et al.*, *MNRAS* **416** (2011) 559
53. A. Bonaldi *et al.*, *MNRAS* **428** (2013) 1845
54. N. S. Kardashev, *Soviet Astronomy* **Vol. 6** (1962) 317
55. M. Murgia, *Publ. of the Astr. Soc. of Australia* **Volume 20, Issue 1** (2002) 19
56. M. Tucci and L. Toffolatti, *AdAst* **2012** (2012) 624987
57. D. Hanson *et al.*, *PRL* **111** (2013) 141301
58. PRISM Collaboration, arXiv:1306.2259 (2013)
59. B. Partridge, M. López-Caniego, R. A. Perley *et al.*, arXiv:1506.02892 (2015)